Pol. J. Environ. Stud. Vol. XX, No. X (XXXX), 1–14
DOI:*10.15244/pjoes/195354* ONLINE PUBLICATION DATE:

Original Research

Penman–Monteith Reference Evapotranspiration Estimation Models, Using Latitude–Temperature Data, in the State of Sinaloa, Mexico

Omar Llanes Cárdenas[1]*, Ernestina Pérez González[1], Mariano Norzagaray Campos[1], Román E. Parra Galaviz[2], Jorge Montiel Montoya[1]

[1]Instituto Politécnico Nacional–Centro Interdisciplinario de Investigación para el Desarrollo Integral Regional (CIIDIR-IPN–SINALOA)
[2]Universidad Autónoma de Sinaloa–Facultad de Ingeniería Mochis (UAS–FIM)

Received: 8 July 2024
Accepted: 28 October 2024

Abstract

The goal is to create regression models estimating the daily Penman–Monteith reference evapotranspiration (PM_R) using latitude–temperature for the state of Sinaloa. The reference evapotranspiration was calculated (1979–2017) by the methods of Penman–Monteith using empirical equations (PM_C), Hargreaves (HA_C), and PM_R. Prior to calculating PM_C, the incident solar radiation (SR) was calculated. From the Acaponeta station (2005–2008, 2011–2013, and 2015–2017), all complete observed variables were obtained: mean temperature, incident solar radiation (SRg), average relative humidity, and average wind speed at a height of 10 m. The data from the eight weather stations were provided by the National Meteorological Service and the National Water Commission. The daily observed Penman–Monteith reference evapotranspiration (PM_O) was calculated. For validation, three simple linear regressions (SLR) were applied: SR vs SRg, PM_C vs PM_O, and PM_R vs PM_O hypothesis tests were applied to each SLR: Pearson correlation (Pr) vs critical Pearson correlation (Pcr). All rP were significantly different from zero (>|0.576|): SRg vs SR (Pr = 0.951), PM_C vs PM_O (Pr = 0.592), and PM_R vs PM_O (Pr = 0.625). This study provides new models that can motivate and support intelligent irrigation in “the breadbasket of Mexico.”

Keywords: reference evapotranspiration, Penman–Monteith, Hargreaves, intelligent irrigation, “the breadbasket of Mexico”

Introduction

Historically, to guarantee the feeding of the world population, agriculture has been the activity that has consumed the greatest amount of water [1]. Approximately 40% of the world’s food depends on activities inherent to agricultural irrigation [2]. This constantly increasing water demand [3] can trigger significant meteorological droughts [4–6], which are accentuated in arid regions [6, 7], where the incident solar radiation (SR) is more intense [8, 9]. Intense SR causes approximately 60% of precipitation to

*e-mail: oma_llanes@yahoo.com.mx
Tel./Fax: +(52) 687-872-9625

return to the atmosphere in the form of evapotranspiration [10, 11], causing these regions to be classified as vulnerable to desertification [12]. For example, in semi-arid regions, agricultural irrigation is a parameter that should trend toward intelligent irrigation [13–16]. To develop intelligent irrigation, valuable information must be available that establishes the relationship between crop growth and water balance [17], in which reference evapotranspiration (ETo) is essential [18]. According to [19] and [20], ETo is the potential evapotranspiration of a hypothetical grass surface with uniform height, well-watered, and active growth, and which depends entirely on climatological variables [9, 21]. According to [9, 22–24], it is always advisable to use empirical equations to estimate ETo by the Penman–Monteith (PM_C) method, even when data is lacking, mainly because it remains the most precise method. Of alternative methods, Hargreaves (HA_C) continues to be the most used, mainly due to its high accuracy/number of variables used ratio [25–27]. However, [26, 27] state that another possible way to estimate ETo by Penman–Monteith is through simple linear regressions (SLR) and simple nonlinear regressions (SNR); PM_R (dependent variable) vs HA_C (independent variable), which more accurately calculates the hydric requirements of crops.

In Mexico, approximately 77% of the volume of the total water resource is allocated to the agricultural sector, and two-thirds of the national territory is characterized by an aridity index ranging from arid to semi-arid [13]. In particular, the state of Sinaloa has a predominantly semi-arid climate [7], and according to [13, 23], this condition predisposes it to focus efforts on the characterization of PM_R, as well as the subsequent design and administration of intelligent irrigation systems [13, 23]. Intelligent irrigation could improve the volumes of yields of Sinaloan crops as well as encourage the conservation of water resources [23, 28].

In this study, daily series (1979–2017) of minimum (Tmin) and maximum (Tmax) temperatures were obtained from seven weather stations in Sinaloa from the National Water Commission (CONAGUA) [29]. PM_C, HA_C, and PM_R were calculated. At another weather station, Acaponeta, observed daily series (2005–2008, 2011–2013, and 2015–2017) were obtained of mean temperature (Tmno), incident solar radiation (SRg), average relative humidity (), and average wind speed at a height of 10 m (). The data for the eight stations were provided by the CONAGUA [29] and CONAGUA–National Meteorological Service (SMN) (CONAGUA–SMN) [30]. At Acaponeta, daily observed Penman–Monteith ETo (PM_O) was calculated. For validation, three SLRs were obtained: SR vs SRg, PM_C vs PM_O, and PM_R vs PM_O. A hypothesis test was applied: Pearson correlation (Pr) vs Pearson critical correlation (Pcr). In the three SLRs, the condition Pr > |Pcr| was met; that is, all Pr were significantly different from zero [31].

The goal was to create PMR estimation models using latitude–temperature data for the state of Sinaloa, Mexico.

Although most of the weather stations for public use in Sinaloa lack the full set of climate variables necessary for the calculation of PM_O [7], in this study, predictive models of PM_R are provided using the variables latitude–temperature. These models can help ensure the feeding of "the breadbasket of Mexico" through intelligent irrigation [13, 23].

Materials and Methods

Study Area

Sinaloa is in the northwest of Mexico (Fig. 1), and because it is the most important agricultural state in Mexico, it is called "the breadbasket of Mexico" [32]. Furthermore, this state is the main producer of export-oriented crops [33] cited by [32]. Due to the planted area and sensitivity to extremes of RH_O–Tmax–Tmin, two of the most important crops in Sinaloa are corn and beans [28].

Data

Daily Maximum (Tmax) and Minimum Temperature (Tmin)

Using data from CONAGUA (https://smn.conagua.gob.mx/es/climatologia/informacion-climatologica/informacion-estadistica-climatologica) [29], daily series of Tmax and Tmin were obtained from 70 weather stations in Sinaloa for the period 1942–2019. These same series were previously obtained by [34]. Through a review of the availability of recent information (< 5% missing data), in this study, it was decided to work with seven weather stations (Culiacán, El Playón, Las Tortugas, Rosario, La Concha, Ixpalino, and Sanalona II) for the period 1979–2017 (Fig. 1).

Imputation of Missing Data, Homogenization of Series, and Determination of the Mean Daily Temperature (Tmn)

Using RStudio software, with the Climatol library [35] and the orthogonal regression method, missing daily data of Tmax and Tmin were estimated by imputation. Using the standard normal homogeneity test (SNHT) [36] method, with Climatol, the series was also homogenized. By means of the semi-sum of the complete and homogeneous series of Tmax and Tmin, the daily series of Tmn was determined.

In general, the greatest thermal extremes were registered in Ixpalino (Tmax = 46.50°C day^{-1}), El Playón and Las Tortugas (Tmin = −6.00°C day^{-1}), and El Playón (Tmn = 38.00°C day^{-1}, Table 1).

Wind Speed at 10 m Height (U_z)

Through the National Oceanic and Atmospheric Administration (NOAA) [37] (https://downloads.psl.noaa.gov/Datasets/ncep.reanalysis2/Monthlies/gaussian_grid/), the monthly series (Jan–Dec) of wind speed at a height of 10 m (U_z) were obtained for the period 1979–2017. Due to the availability of satellite information, U_z was obtained for only two coordinates in the state of Sinaloa: 1) 25°43′14″ N by 108°45′00″ W and 2) 23°55′42″ N by 106°46′48″ W.

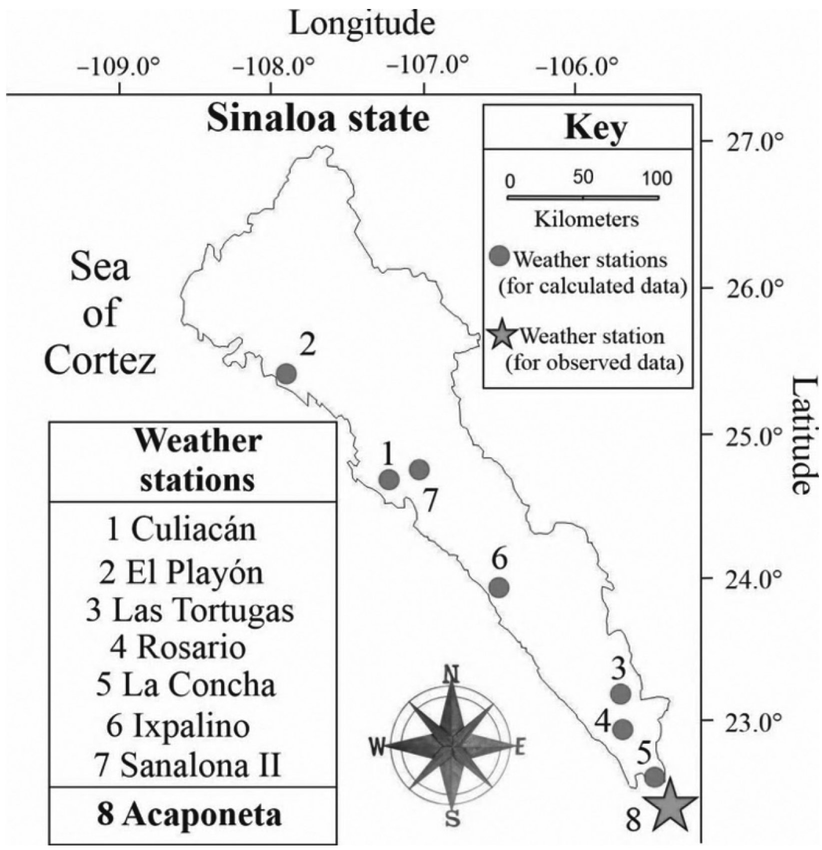

Fig. 1. Study area, Sinaloa state.

Table 1. Maximum, minimum, and average values of the maximum (Tmax), minimum (Tmin) and mean (Tmn) temperatures, in Sinaloa, for the period 1979–2017.

Weather station	Statistical variable	Tmax (°C day^{-1})	Tmin (°C day–1)	Tmn (°C day^{-1})
Culiacán	Maximum	45.50	29.80	35.00
	Minimum	15.50	2.00	11.00
	Average	33.29	19.30	26.30
El Playón	Maximum	45.50	37.00	38.00
	Minimum	13.00	–6.00	8.75
	Average	31.54	16.52	24.03
Las Tortugas	Maximum	41.50	28.00	33.50
	Minimum	17.50	–6.00	11.00
	Average	33.56	16.87	25.21
Rosario	Maximum	41.00	31.00	35.00
	Minimum	17.00	1.40	14.00
	Average	32.66	18.86	25.76
La Concha	Maximum	43.50	30.00	34.90
	Minimum	19.00	4.00	14.00
	Average	33.86	20.17	27.02
Ixpalino	Maximum	46.40	28.50	34.65
	Minimum	19.00	–1.30	11.70
	Average	35.08	17.34	26.21

Weather station	Statistical variable	Tmax (°C day^{-1})	Tmin (°C day–1)	Tmn (°C day^{-1})
Sanalona II	Maximum	43.00	27.20	34.35
	Minimum	17.00	–5.00	8.25
	Average	33.94	15.19	24.56

Empirical Equations to Estimate Penman–Monteith Reference Evapotranspiration, Calculated with Missing Data (PM_C) and Observed Data (PM_O)

Wind Speed at 2 m Height (U_2)

Although [9, 38] states that wind speed is not very relevant for estimating PM_C in semi-arid regions, in this study, using Equation 1, the wind speed was obtained at a height of 2 m (U_2) [19, 22].

$$U_2 = U_z \cdot \left[\frac{4.87}{\ln \cdot (67.8 \cdot z - 5.42)}\right], \quad (1)$$

where U_2 = monthly average wind speed at a height of 2 m (m s^{-1}), U_z = average wind speed measured at a height of 10 m (m s^{-1}), and z = measurement height of U_z (m).

Since PM_C is the international standard because of its greater measurement accuracy [9], in this study, PM_C was estimated daily using Equations 2–10. These equations, which are recommended by [19, 22] when there are missing data, are given as follows:

$$e_{aC} = 0.6108 \cdot \exp\left(\frac{17.27 \cdot \mathrm{Tmin}}{\mathrm{Tmin} + 237.3}\right), \quad (2)$$

where e_{aC} = calculated actual vapor pressure and Tmin = daily minimum air temperature (°C).

$$e_s = \left(0.6108 \cdot \exp\frac{17.27 \cdot \mathrm{Tmn}}{\mathrm{Tmn} + 237.3}\right), \quad (3)$$

where e_s = saturation vapor pressure (kPa) and Tmn = daily mean air temperature (°C).

$$\Delta = \frac{4098 \cdot \left[0.6108 \cdot \exp\frac{17.27 \cdot \mathrm{Tmn}}{\mathrm{Tmn}+237.3}\right]}{(\mathrm{Tmn}+237.3)^2}, \quad (4)$$

where Δ = slope of the saturated vapor pressure curve (kPa $°C^{-1}$).

$$\mathrm{SR} = K_{RS} \cdot (\mathrm{Tmax} - \mathrm{Tmin})^{0.5} \cdot \mathrm{Ra}, \quad (5)$$

where SR = calculated incident solar radiation (MJ m^{-2} day^{-1}), KRS = solar radiation adjustment coefficient (dimensionless), with a value of 0.16 for continental conditions and 0.19 for coastal conditions (in this study, KRS = 0.16 was used), Tmax = maximum daily air temperature (°C), and Ra = extraterrestrial solar radiation (obtained through tabulated values with respect to latitude, MJ m^{-2} day^{-1}).

$$\mathrm{SRo} = 0.75 \cdot \mathrm{Ra}, \quad (6)$$

where SRo = incident solar radiation with clear sky (MJ m^{-2} day^{-1}).

$$\mathrm{Rnl} = \left[(\sigma \cdot \mathrm{TmnK}^4) \cdot (0.34 - 0.14 \cdot e_a^{0.5}) \cdot \left(1.35 \cdot \frac{\mathrm{SR}}{\mathrm{SRo}} - 0.35\right)\right] \quad (7)$$

where Rnl = net longwave radiation (MJ m^{-2} day^{-1}), σ = Stefan–Boltzmann constant (0.4903×10^{-8} MJ K^{-4} m^{-2} day^{-1}) and TmnK = mean daily air temperature ($°K^4$).

$$\mathrm{Rns} = 0.77 \cdot \mathrm{SR}, \quad (8)$$

where Rns = net shortwave radiation (MJ m^{-2} day^{-1}).

$$\mathrm{Rn} = \mathrm{Rns} - \mathrm{Rnl}, \quad (9)$$

where Rn = net radiation (MJ m^{-2} day^{-1}).

$$PM_C \text{ and } PM_O = \frac{0.408 \cdot \Delta \cdot (\mathrm{Rn} - \mathrm{G})}{\Delta + \gamma \cdot (1 + 0.34 \cdot U_2)} + \frac{\gamma \cdot \frac{900}{\mathrm{Tmn} + 273} \cdot U_2 \cdot (e_s - e_{aC})}{\Delta + \gamma \cdot (1 + 0.34 \cdot U_2)} \quad (10)$$

where PM_C = Penman–Monteith reference grass evapotranspiration (mm day^{-1}, calculated with missing data), PM_O = Penman–Monteith observed grass reference evapotranspiration (mm day^{-1}, at the Acaponeta station), G = soil heat flux density (MJ m^{-2} day^{-1}, null for daily estimates), and γ = psychrometric constant (0.067 kPa°C^{-1}; tabulated value by [19, 22], for stations with altitudes ranging from 0 to 100 masl).

Calculated Hargreaves Reference Evapotranspiration (HAC, Alternative Method Used)

When the absence of data does not allow Equation 10 to be used, [25] recommends the use of Expression 11 to estimate HA_C, which is widely recommended worldwide due to the high ratio accuracy/number of variables used.

$$HA_C = 0.0023 \cdot Ra \cdot (Tmn + 17.8) \cdot (Tmax - Tmin)^{0.5}, \tag{11}$$

where HA_C = Hargreaves reference evapotranspiration (mm day^{-1}).

PM_C and HA_C were also calculated as monthly (Jan–Dec), seasonal (Mar–Aug), and annual (Jan–Dec) averages.

Pre-Validation

Normality Test and Correlation Coefficients

A Shapiro–Wilk normality test was applied to all PM_C and HA_C series [39]. To find out whether PM_C and HA_C were significantly correlated, a Pr was applied to the series that presented normality, and a Spearman correlation (Sr) was applied to the series that did not present normality.

Simple Linear Regressions (SLR) and Simple Nonlinear Regressions (SNR)

To generate sensitive models [7] to predict PM_R (dependent variable) based on HA_C (independent variable), SLR were initially fitted (Equation 12). A Shapiro–Wilk normality test was applied to the SLR residuals. When the residuals were not normal, an SNR (10 different functions) was applied, fitting a curvilinear estimate. Of the 10 functions, the following were chosen: a) exponential function (monthly series, Equation 13) and potential function (seasonal series, Equation 14), which were selected due to the highest R^2 recorded.

$$PM_R = a + b \cdot HA_C, \tag{12}$$

$$PM_R = a \cdot e^{b \cdot HA_C}, \tag{13}$$

$$PM_R = a \cdot {HA_C}^{b}, \tag{14}$$

where e = Euler number (2.7182) and a, b = regression coefficients that describe the relationship between PM_R and HA_C.

Hypothesis Test

For each SLR and SNR, the Pr and Sr were obtained by the square root of R^2. To find out if each Pr and Sr were significantly different from zero, hypothesis tests were applied [31, 40]. Each Pr and Sr were compared with a Pcr = |0.316| (Equation 15) and a critical Spearman correlation coefficient (Scr = 0.318, Equation 16).

$$Pcr = \sqrt{\frac{\frac{t_c^2}{df}}{\frac{t_c^2}{df}+1}}, \tag{15}$$

where t_c = critical value of the student t statistic and df = degrees of freedom (n–2).

$$Scr = \pm z\sqrt{n-1}, \tag{16}$$

where z = 1.96, n = 39 (for the period 1979–2017).

The design of the hypotheses is shown in Equations 17–18:

$$H_o: Pr \geq |Pcr| \text{ and } Sr \geq |Scr| \therefore Pr \text{ and } Sr \neq 0 \text{ (null hypothesis)}, \tag{17}$$

$$H_1: Pr < |Pcr| \text{ and } Sr < |Scr| \therefore Pr \text{ and } Sr = 0 \text{ (alternative hypothesis)}. \tag{18}$$

Also, the root mean square error (RMSE) between PM_C and PM_R was calculated.

Validation

Using the CONAGUA–SMN database (https://smn.conagua.gob.mx/tools/GUI/sivea_v3/sivea.php) [30], the following observed data were obtained from the Acaponeta station: Tmn_O, U_{ZO}, SRg, and RH_O, for the periods 2005–2008, 2011–2013, and 2015–2017. PM_O was calculated, reapplying Equations 1, 3–4, 6–10, and 19.

$$e_{aO} = \frac{RH_O}{100} \cdot e_s, \tag{19}$$

where e_{aO} = observed actual vapor pressure and RH_O = observed mean daily relative humidity (%).

Three SLRs were applied: 1) SR (La Concha) vs SRg (Acaponeta), 2) PM_C (La Concha) vs PM_O (Acaponeta), and 3) PM_R (La Concha) and PM_O (Acaponeta). A Shapiro–Wilk normality test was applied to the residuals of the three SLRs. From each SLR, Pr = $(R^2)^{0.5}$ was obtained. To find out if Pr was significantly different from zero, another hypothesis test was carried out between Pr vs Pcr = |0.576|

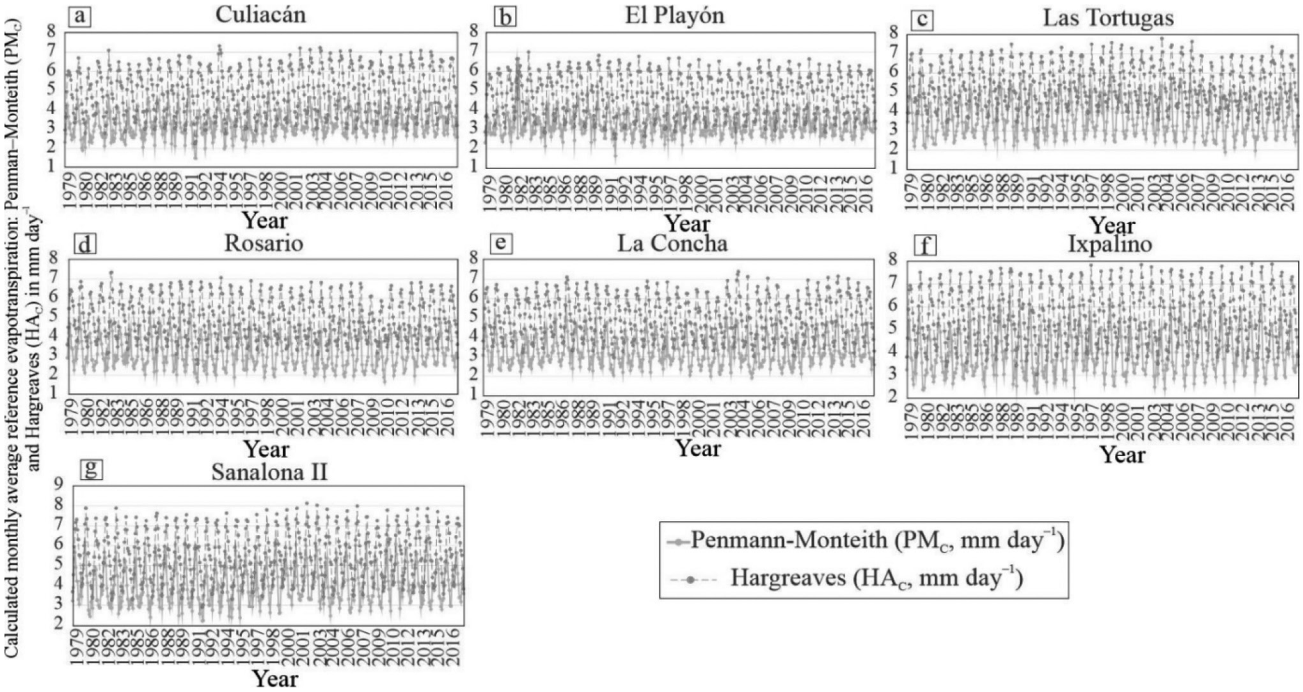

Fig. 2. Calculated monthly average reference evapotranspiration: Penman–Monteith (PM_C) and Hargreaves (HA_C) methods for the period 1979–2017 (mm day^{-1}).

(for n = 12). Finally, the RMSE values were calculated between the calculated and observed values of the three SLRs. The pre-validation and validation were adaptations of the development by [7].

Software Used

To carry out this research, the following programs were used: RStudio version 4.3.0, Past version 4.08, XLstat version 2023, Panoply version 5.2.6, and CorelDRAW version 2019.

Results and Discussion

Calculated Monthly Average Reference Evapotranspiration: Penman–Monteith (PM_C) and Hargreaves (HA_C) Methods

The average ETo ranged from PM_C = 1.483 mm day^{-1} in 1992 (Culiacán–Jan, Fig. 2a)) to PM_C = 6.656 mm day^{-1} in 1982 (El Playón–May, Fig. 2b)); and from HA_C = 2.256 mm day^{-1} in 1991 (Culiacán–Dec, Fig. 2a)) to HA_C = 8.133 mm day^{-1} in 2002 (Sanalona II–May, Fig. 2g)). The results of Fig. 2a) are similar to those reported by [41], who found a range from PM_C = 3.0 mm day^{-1} to PM_C = 5.8 mm day^{-1} for the Culiacán valley in the period 2013–2014. The variation between PM_C vs HA_C ranged from RMSE = 1.861 mm day^{-1} (El Playón, Fig. 2b)) to RMSE = 1.972 mm day^{-1} (Culiacán, Fig. 2a)), that is, ETo presents a tendency towards underestimation of PM_C and overestimation of HA_C (RMSE > 0.3 mm day^{-1}) [9].

Normality Test for the Calculated Average Reference Evapotranspiration: Penman–Monteith (PM_C) and Hargreaves (HA_C) Methods

Monthly (Jan–Dec), Seasonal (Mar–Aug), and Annual (Jan–Dec) Series

For PM_C–Ixpalino in all months (Jan–Dec), p(normal), and W ranged from 0.090 to 0.623 and from 0.951 to 0.978, respectively (Fig. 3a)). In total, 37 monthly series did not present normality; PM_C = 15 series and HA_C = 22 series (Fig. 3a)). The seasonal series (Mar–Aug) that did not present normality [p(normal) < 0.05] were PM_C–El Playón [p(normal) = 7.8×10^{-5}], HA_C–El Playón [p(normal) = 1.7×10^{-6}], HA_C–Las Tortugas [p(normal) = 0.003], and HA_C–Rosario [p(normal) = 0.008, Fig. 3b)]. The annual series (Jan–Dec) without normality were PM_C–El Playón [p(normal) = 2.3×10^{-4}], HA_C–El Playón [p(normal) = 9.4×10^{-7}], HA_C–Las Tortugas [p(normal) = 0.006] and HA_C–Ixpalino [p(normal) = 0.018, Fig. 3b)]. According to [42], the results of the PM_C–Ixpalino series (Fig. 3a)) present normality. According to [43], in the results of Fig. 3b), the seasonal series (Mar–Aug) that did not present normality were: PM_C–El Playón, HA_C–El Playón, HA_C–Las Tortugas, and HA_C–Rosario, because they did not present the condition of p(normal) > 0.05. According to [43, 44], the annual series (Jan–Dec) that did not present normality were PM_C–El Playón, HA_C–El

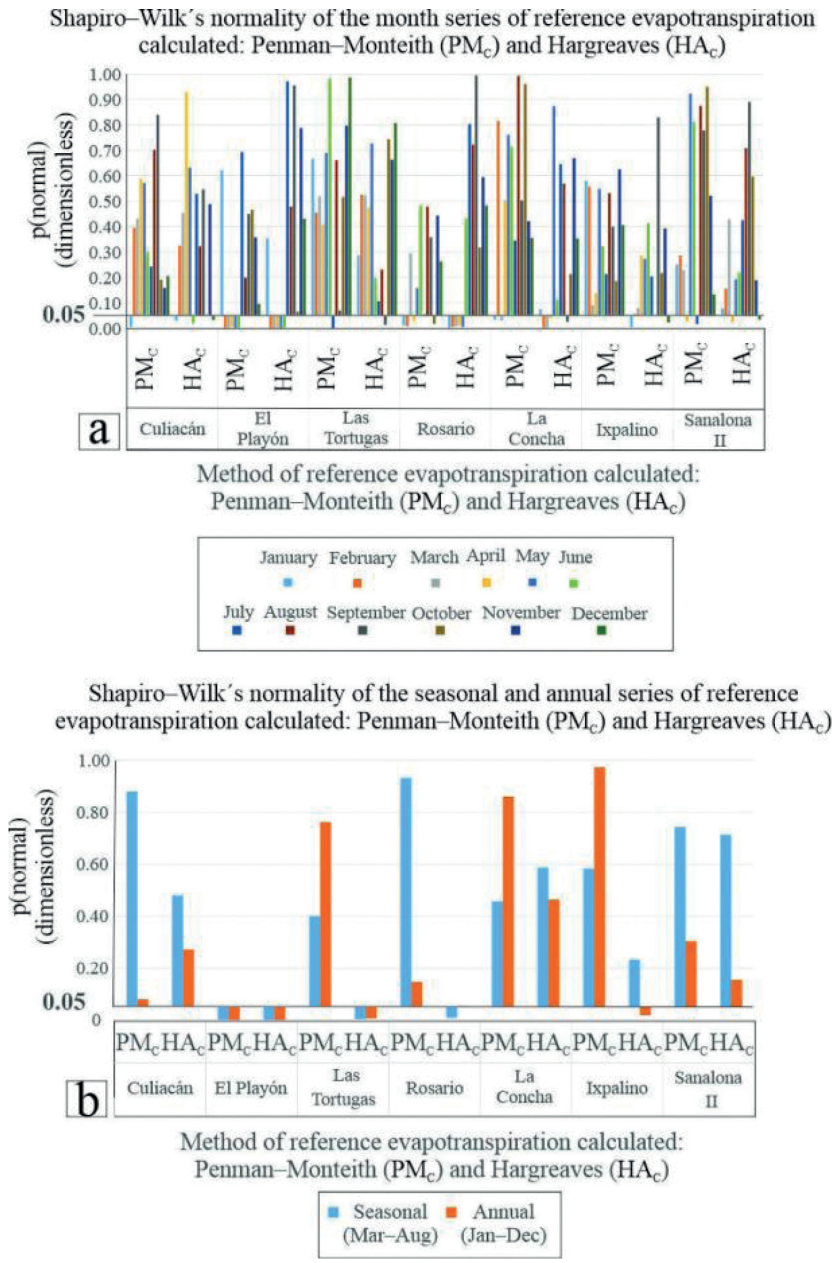

Fig. 3. Normality of the monthly series (Jan–Dec) of calculated reference evapotranspiration: Penman–Monteith (PM_C) and Hargreaves (HA_C) methods, for the period 1979–2017 (dimensionless).

Playón, HA_C–Las Tortugas, and HA_C–Ixpalino, this is due to $p(\text{normal}) < 0.05$.

Pearson (rP) and Spearman (rS) Correlations of Calculated Average Reference Evapotranspiration: Penman–Monteith (PMC) and Hargreaves (HAC) Methods

Monthly Correlations (Jan–Dec)

As shown in Table 2, the correlations ranged from rP = 0.443 (El Playón–Jul) to rP = 0.929 (Las Tortugas–Jan). All rP and rS were significantly different from zero ($rP > rcP = |0.316|$ and $rS > rcS = |0.318|$). According to [31, 40], the results of Table 2 establish the significant monthly relationship (Jan–Dec) of PM_C vs HA_C, so monthly modeling of PM_R is appropriate (Equations 12–14), applying SLR and SNR, as recommended by [19, 22] and applied by [27, 45].

Seasonal (Mar–Aug) and Annual (Jan–Dec) Correlations

As shown in Table 3, all seasonal (Mar–Aug) and annual (Jan–Dec) rP and rS were significantly different from zero ($rP > rcP = 0.316$ and $rS > rcS = 0.318$). Seasonal correlations (Mar–Aug) ranged from rP = 0.693 (Sanalona

Table 2. Pearson (rP) and Spearman (rS) correlations of the calculated monthly average reference evapotranspiration (Jan–Dec): Penman–Monteith (PMC) and Hargreaves (HAC) methods (dimensionless).

Type of correlation	Weather station	Jan	Feb	Mar	Apr	May	Jun	Jul	Aug	Sep	Oct	Nov	Dec
Pearson (rP)	Culiacán		0.895	0.848	0.869	0.780		0.639	0.781	0.908	0.867	0.865	
	El Playón	0.896						0.443	0.691	0.888	0.841	0.845	0.840
	Las Tortugas	0.929	0.878	0.808	0.772	0.734	0.848		0.831		0.850	0.829	0.866
	Rosario						0.890	0.793	0.852	0.913		0.857	0.842
	La Concha					0.831	0.839	0.753	0.820		0.850	0.811	0.831
	Ixpalino		0.887	0.856	0.812	0.566	0.822	0.473	0.754	0.867	0.853	0.842	
	Sanalona II	0.920	0.892	0.864		0.560	0.722		0.702	0.846	0.836	0.877	
Spearman (rS)	Culiacán	0.846					0.719						0.845
	El Playón		0.767	0.682	0.816	0.725	0.749						
	Las Tortugas							0.656		0.798			
	Rosario	0.793	0.820	0.721	0.790	0.757					0.832		
	La Concha	0.856	0.809	0.866	0.859					0.843			
	Ixpalino	0.916											0.750
	Sanalona II				0.740			0.551					0.837

n = 39; rcP = |0.316|; rcS = |0.318|

Table 3. Pearson (rP) and Spearman (rS) correlations of calculated seasonal (Mar–Aug) and annual (Jan–Dec) average reference evapotranspiration: Penman–Monteith (PMC) and Hargreaves (HAC) methods (dimensionless).

Type of correlation	Weather station	Seasonal (Mar–Aug)	Annual (Jan–Dec)
Pearson (rP)	Culiacán	0.852	0.895
	El Playón		
	Las Tortugas		
	Rosario		0.865
	La Concha	0.907	0.921
	Ixpalino	0.698	
	Sanalona II	0.693	0.848
Spearman (rS)	Culiacán		
	El Playón	0.794	0.831
	Las Tortugas	0.773	0.854
	Rosario	0.823	
	La Concha		
	Ixpalino		0.839
	Sanalona II		

n = 39; rcP = |0.316|; rcS = |0.318|

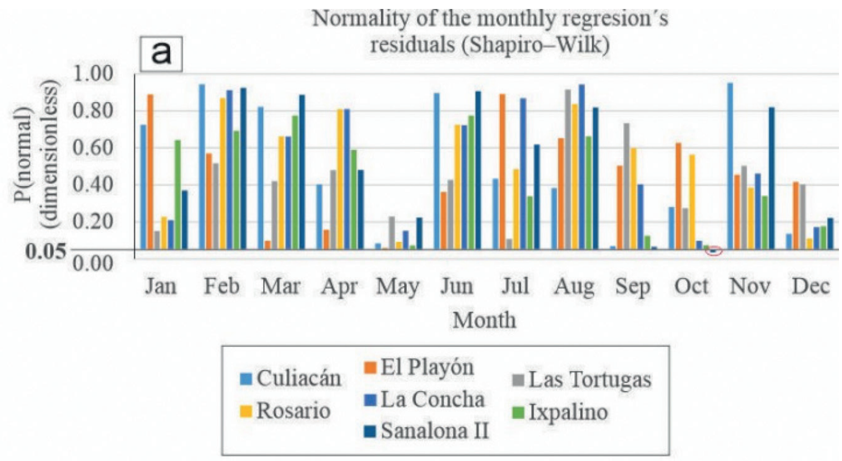

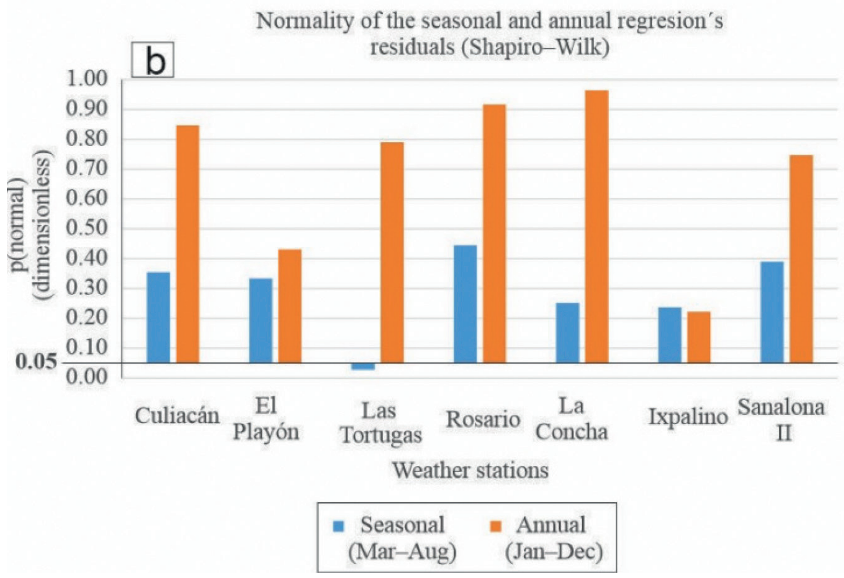

Fig. 4. Normality of regression residuals between reference evapotranspiration calculated from Penman–Monteith (PM_R) and Hargreaves (HA_C): a) monthly (Jan–Dec) and b) seasonal (Mar–Aug) and annual (Jan–Dec) (dimensionless).

II) to rP = 0.907 (La Concha). The annual correlations (Jan–Dec) ranged from rS = 0.831 (El Playón) to rP = 0.921 (La Concha). Because all the correlations in Table 3 were significant [31, 40], SLR and SNR can be applied to estimate PM_R with a seasonal (Mar–Aug) and annual (Jan–Dec) scale, with HA_C as the independent variable [27–45].

Linear (SLR) and Simple Nonlinear Regressions (SNR) of Calculated Average Reference Evapotranspiration: Penman–Monteith (PM_R, dependent Variable) and Hargreaves (HA_C, Independent Variable) Methods

Normality Test of Monthly (Jan–Dec), Seasonal (Mar–Aug), and Annual (Jan–Dec) Residuals

The only series of monthly residuals (Jan–Dec) that did not present normality was Sanalona II–Oct [p(normal) = 0.046 and W = 0.942, Fig. 4a)]. In the normal monthly series, the p(normal) values ranged from 0.059 (El Playón–May) to 0.951 (Culiacán–Nov, Fig. 4a)). As seen in Fig. 4b), Las Tortugas for the seasonal period (Mar–Aug) [p(normal) = 0.028 and W = 0.936] was the only series that did not register normality. In the normal seasonal series, the p(normal) values ranged from 0.237 (Ixpalino) to 0.445 (Rosario). In the normal annual series, the p(normal) values ranged from 0.221 (Ixpalino) to 0.964 (La Concha). According to [43] in the results of Fig. 4b), and for the seasonal period (Mar–Aug), the only series that did not present normality was Las Tortugas, because $p < 0.05$. All series that did present the condition of $p > 0.05$ were considered normal series [42].

Monthly Coefficients and Goodness of Fit (Jan–Dec)

The fit ranged from $R^2 = 0.196$ (rP = 0.443, El Playón–Jul) with RMSE = 0.274 mm day^{-1} to $R^2 = 0.863$ (rP = 0.929, Las Tortugas–Jan) with RMSE = 0.218 mm day^{-1} (Table 4). For

Table 4. Monthly regression coefficients to estimate calculated reference evapotranspiration: Penman–Monteith (PM_R, dependent variable) and Hargreaves (HA_C, independent variable) (dimensionless).

Month	Type of coefficient of the equation	Coefficients of each equation by weather station						
		Culiacán	El Playón	Las Tortugas	Rosario	La Concha	Ixpalino	Sanalona II
Jan	a	–1.330	–1.864	–2.877	–1.942	–2.116	–3.322	–2.851
Feb		–2.734	–2.612	–2.359	–2.335	–1.838	–3.967	–3.833
Mar		–2.178	–2.952	–2.485	–2.225	–2.486	–3.926	–3.479
Apr		–3.045	–2.405	–3.781	–3.793	–3.274	–4.429	–4.668
May		–1.781	–2.705	–2.400	–2.113	–3.364	–3.021	–0.777
Jun		–1.495	–1.551	–2.915	–2.650	–1.694	–5.048	–3.747
Jul		0.105	–0.313	–1.712	–1.042	–1.269	0.286	–0.100
Aug		–0.951	–1.938	–1.229	–1.137	–1.164	–1.935	–1.079
Sep		–1.784	–1.655	–0.914	–0.851	–0.966	–2.229	–2.295
Oct		–2.350	–2.887	–2.354	–1.469	–1.935	–2.901	**0.530**
Nov		–2.440	–2.280	–2.558	–1.947	–2.062	–2.521	–3.186
Dec		–1.409	–0.956	–2.661	–1.763	–1.673	–2.705	–2.731
Jan	b	1.250	1.456	1.639	1.368	1.426	1.779	1.714
Feb		1.488	1.486	1.379	1.340	1.228	1.716	1.733
Mar		1.193	1.368	1.266	1.190	1.227	1.507	1.460
Apr		1.192	1.094	1.314	1.310	1.224	1.402	1.454
May		0.883	1.033	0.988	0.936	1.120	1.069	0.782
Jun		0.782	0.798	1.009	0.974	0.816	1.302	1.113
Jul		0.526	0.605	0.829	0.709	0.751	0.515	0.576
Aug		0.664	0.852	0.708	0.691	0.700	0.832	0.688
Sep		0.885	0.883	0.704	0.686	0.717	0.963	0.976
Oct		1.140	1.293	1.128	0.932	1.044	1.239	**0.366**
Nov		1.388	1.409	1.364	1.209	1.251	1.382	1.570
Dec		1.259	1.179	1.561	1.295	1.287	1.610	1.670

Plain Simple linear regression (SLR)
Bold Simple nonlinear regression (SNR)

the SNR–exponential function (Sanalona II–Oct, Table= 4), $R^2 = 0.706$ (rS = 0.840 > rcS = |0.318|). All RLS (Table 4) exceeded rcP = |0.316| [31, 40] (significant correlation) and did not register a trend towards underestimation or overestimation (RMSE < 0.300 mm day^{-1}) [9]. In Table 4 and for Sanalona II–Oct (SNR–exponential function), the results were rS = 0.840 > rcS = |0.318| [31, 40] (significant correlation) [31, 40]. The methodology of Table 4 was applied to obtain more accurate estimates [19, 22] and was previously applied by [26, 27].

Coefficients and Seasonal (Mar–Aug) and Annual (Jan–Dec) Goodness of Fit

Seasonal fit (Mar–Aug, Table 5) ranged from $R^2 = 0.480$ (rP = 0.693, Sanalona II) with

Table 5. Seasonal and annual regression coefficients, to estimate calculated reference evapotranspiration: Penman–Monteith (PM_R, dependent variable) and Hargreaves (HA_C, independent variable) (dimensionless).

Weather station	Seasonal (Mar–Aug)		Annual (Jan–Dec)	
	a	b	a	b
Culiacán	–0.916	0.761	–1.182	0.888
El Playón	–2.216	0.992	–2.304	1.141
Las Tortugas	**0.352**	**1.328**	–1.365	0.947
Rosario	–1.428	0.853	–0.124	0.841
La Concha	–2.005	0.945	–1.771	1.001
Ixpalino	–3.036	1.114	–3.994	1.420
Sanalona II	–1.358	0.869	–2.873	1.233

Plain Simple linear regression (SLR)
Bold Simple nonlinear regression (SNR)

RMSE = 0.156 mm day^{-1} to R^2 = 0.823 (rP = 0.907, La Concha) with RMSE = 0.117 mm day^{-1}. Annual fit (Jan–Dec) ranged from R^2 = 0.719 (rP = 0.848, Sanalona II) with RMSE = 0.112 mm day^{-1} to R^2 = 0.848 (rP = 0.921, La Concha) with RMSE = 0.082 mm day^{-1}. For the SNR–potential function (Las Tortugas–seasonal, Table 5), the fit was R^2 = 0.699 (rS = 0.836 > rcS = |0.318|). All SLR (seasonal and annual, Table 5) exceeded rcP = |0.316| [31, 40] (significant correlation) and showed no trend towards underestimation or overestimation (RMSE < 0.300 mm day^{-1}) [9]. These results are in agreement with [19, 22], who state that PM_R models are more accurate than when only Equations 1–10 (PM_C) are used. [46] also state that HA_C estimation is the most recommended method when data is not available to estimate PM_C.

Validation

Simple Linear Regressions (SLR) between Calculated and Observed Values from: 1) Incident Radiation (SR vs SRg), 2) Penman–Monteith Reference Evapotranspiration, Calculated with Equations (PM_C vs PM_O), and 3) Calculated with Regressions (PM_R vs PM_O)

All the monthly average SLR (Fig. 5a)–5c)) recorded rP significantly different from zero (rP > rcP = |0.576|, for n = 12). Specifically for SR vs SRg, the measures of fit were: R^2 = 0.905, rP = 0.951, and RMSE = 0.684 mm day^{-1} (Fig. 5a)). In PM_C vs PM_O, the measures of fit were R^2 = 0.350, rP = 0.592, and RMSE = 0.590 mm day^{-1} (Fig. 5b)). For PM_R vs PM_O, the measures of fit were R^2 = 0.391, rP = 0.625, and RMSE = 0.578 mm day^{-1} (Fig. 5c)). The residuals of the three SLR presented normality: p(normal) = 0.193 and W = 0.907 (Fig. 5a)), p(normal) = 0.344 and W = 0.927 (Fig. 5b)), and p(normal) = 0.464 and W = 0.937 (Fig. 5c)). In validation, the three SLRs (Fig. 5a)–5c)) performed well (RMSE < 1.0 mm día^{-1}) [47]. In this study, SR was highly influential (approximately 90.5%) for estimating PM_C, which agrees with [8], who points out that SRg in Sinaloa is decisive for the estimation of PM_C. According to the results of PM_C vs PM_O (Fig. 5b)), Equations 1–10 were reliable and sensitive for estimating PM_C, even when the series presented missing data [9, 48, 49]. The results of Fig. 5c) and, according to [19, 22, 26, 27], the models of this study are also reliable and sensitive for predicting PM_R. Finally, because the residuals of the three SLRs (Fig. 5a)–5c)) presented normality, the SLR is an appropriate statistical tool to use for comparison of calculated and observed data [7].

Conclusions

Due to the lack of data variables from weather stations in Sinaloa, PM_C, and HA_C were estimated with the use of equations. PM_C presented trends toward underestimation, and HA_C presented trends toward overestimation. For the first time in Sinaloa, monthly (Jan–Dec), seasonal (Mar–Aug), and annual (Jan–Dec) SLR and SNR were generated to estimate PM_R (dependent variable) using HA_C (independent variable). Although the equations are a good tool to estimate PM_C, the use of PM_R estimation models is more precise (without trends of underestimation or overestimation). To try to improve the fit of PM_R vs PM_O, in future studies, it is recommended to estimate PM_R using any other alternative method for ETo, for example, Thornwaite, Priestley–Taylor, Valiantzas, Makkink, Schendel, Jensen, or Turc, among other methods. Knowledge of PM_R in Sinaloa can contribute to facilitating the calculation of crop evapotranspiration, which can

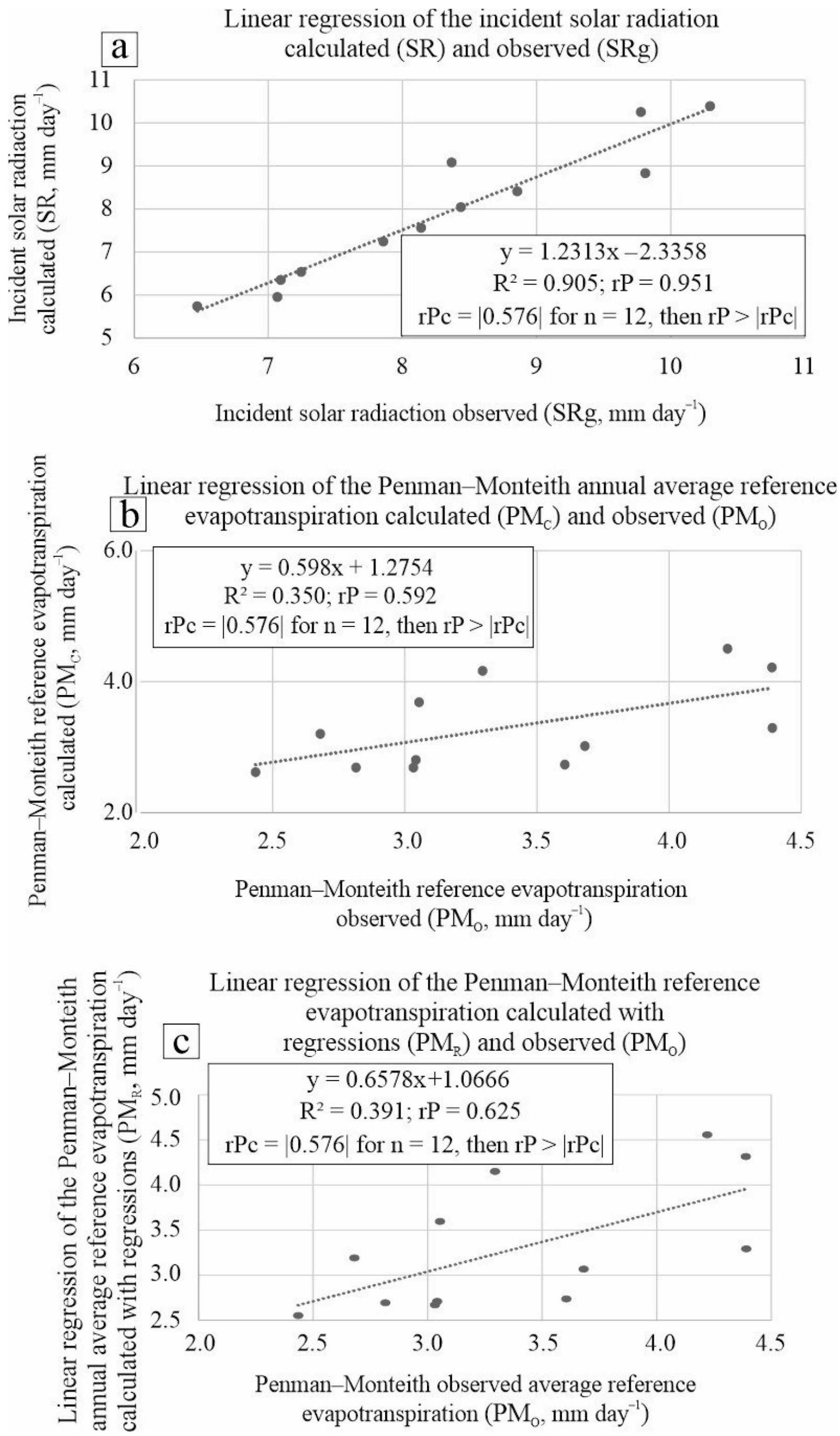

Fig. 5. Regressions of calculated and observed values: a) incident solar radiation (SR vs SRg, mm day^{-1}), b) Penman–Monteith reference evapotranspiration, calculated with equations (PM_C vs PM_O, mm day^{-1}) and c) same as b), but calculated with regressions (PM_R vs PM_O, mm day^{-1}).

enable the design of intelligent irrigation plans that are efficient, sustainable, and affordable. The PM_R models of this study are also a valuable tool when complete climate series are lacking, which are necessary for the calculation of PM_O, since in this study to obtain PM_R only latitude–temperature is required. These predictive models can also help ensure, in the near future, the feeding of the population of "the breadbasket of Mexico," specifically through the relationship between less irrigation water/greater sustainability of food production.

Acknowledgements

This research was financially supported by Secretariat of Investigation and Postgraduate Studies of the National Polytechnic Institute (SIP-IPN) though projects 20231577 and 20240953.

Conflict of Interest

The authors declare no conflict of interest.

References

1. RIBEIRO V.P., DESUÓ N.L., MARQUES P.A.A., ACHCAR J.A., JUNQUEIRA A.M., CHINATTO A.W., JR. JUNQUEIRA C.C.M., MACIEL C.D., BALESTIERI J.A.P. A Stochastic Bayesian Artificial Intelligence Framework to Assess Climatological Water Balance under Missing Variables for Evapotranspiration Estimates. Agronomy. **13**, 2970, **2023**.
2. RAHEEM A., AHMAD I., ARSHAD A., LIU J., REHMAN Z.U., SHAFEEQUE M., RAHMAN M.M., SAIFULLAH M., IQBAL U. Numerical Modeling of Groundwater Dynamics and Management Strategies for the Sustainable Groundwater Development in Water-Scarce Agricultural Region of Punjab, Pakistan. Water. **16**, 34, **2024**.
3. UNITED NATIONS, DEPARTMENT OF ECONOMIC AND SOCIAL AFFAIRS, POPULATION DIVISION. World Population Prospects. **2022**.
4. YU X.J., ZHANG L.X., ZHOU T.J., ZHENG J.H. Assessing the performance of CMIP6 models in simulating droughts across global drylands. Advances in Atmospheric Sciences. **41** (2), 193, **2024**.
5. ABEL D., ZIEGLER K., GBODE I.E., WEBER T., AJAYI O.V., TRAORÉ S.B., PAETH H. Robustness of climate indices relevant for agriculture in Africa deduced from GCMs and RCMs against reanalysis and gridded observations. Climate Dynamics. **62**, 1077, **2024**.
6. CARDOSO DO VALE T.M., CONSTANTINO S.M.E., BEZERRA C.J., BARBOSA A.L.M., BEZERRA B.G., TÔRRES R.D., RODRIGUES M.P. Climate and water balance influence on agricultural productivity over the Northeast Brazil. Theoretical and Applied Climatology. **155**, 879, **2024**.
7. LLANES C.O., NORZAGARAY C.M., GAXIOLA A., PÉREZ G.E., MONTIEL M.J., TROYO D.E. Sensitivity of four indices of meteorological drought for rainfed maize yield prediction in the state of Sinaloa, Mexico. Agriculture. **12** (4), 525, **2022**.
8. GONZÁLEZ C.J.M., CERVANTES O.R., OJEDA B.W., LÓPEZ C.I. Predicción de la evapotranspiración de referencia mediante redes neuronales artificiales. Ingeniería Hidráulica de México. **23** (1), 127, **2008**.
9. SENTELHAS P.C., GILLESPIE T.J., SANTOS E.A. Evaluation of FAO Penman–Monteith and alternative methods for estimating reference evapotranspiration with missing data in Southern Ontario, Canada. Agricultural Water Management. **97** (5), 635, **2010**.
10. ZHANG J., ZHOU X., YANG S., AO Y. Spatiotemporal Variations in Evapotranspiration and Their Driving Factors in Southwest China between 2003 and 2020. Remote Sensing. **15**, 4418, **2023**.
11. NIKOLAOU G., NEOCLEOUS D., MANES A., KITTA E. Calibration and validation of solar radiation-based equations to estimate crop evapotranspiration in a semi-arid climate. International Journal of Biometeorology. **68**, 1, **2024**.
12. SEKHAR S.M., PRASAD R.S., MAITY R. Climate change may cause oasification or desertification both: an analysis based on the spatio-temporal change in aridity across India. Theoretical and Applied Climatology. **155**, 1167, **2024**.
13. ESPINOSA E.B., FLORES M.H., HERNÁNDEZ R.A., CARRILLO F.G. Diseño de un sistema de riego hidrante parcelario con los los métodos por turnos y Clement: análisis técnico económico. Terra Latinoamericana. **34** (4), 431, **2016** [In Spanish].
14. ZHAO L., WANG Y., SHI Y., ZHAO X., CUI N., ZHANG S. Selecting essential factors for predicting reference crop evapotranspiration through tree-based machine learning and Bayesian optimization. Theoretical and Applied Climatology. **155,** 2953, **2024**.
15. PEREIRA S.L., PAREDES P., OLIVEIRA M.C., MONTOYA F., LÓPEZ U.R., SALMAN M. Single and basal crop coefficients for estimation of water use of tree and vine woody crops with consideration of fraction of ground cover, height, and training system for Mediterranean and warm temperate fruit and leaf crops. Irrigation Science. **42** (6), 1019, **2023**.
16. KIRAGA S., PETERS R.T., MOLAEI B., EVETT S.R., MAREK G. Reference Evapotranspiration Estimation Using Genetic Algorithm-Optimized Machine Learning Models and Standardized Penman–Monteith Equation in a Highly Advective Environment. Water. **16** (1), 12, **2024**.
17. PENG X., LIU X., WANG Y., CAI H. Evapotranspiration Partitioning and Estimation Based on Crop Coefficients of Winter Wheat Cropland in the Guanzhong Plain, China. Agronomy. **13**, 2982, **2023**.
18. FARMER W., STRZEPEK K., SCHLOSSER A.C., DROOGERS P., GAO X. A method for calculating reference evapotranspiration on daily time scales. Global Sciece Policy Change MIT. **195**, 1, **2011**.
19. ALLEN R.G., PEREIRA L.S., RAES D., SMITH M. Evapotranspiración del cultivo: Guías para la determinación de los requerimientos de agua de los cultivos. Ed. FAO. **1998a** [In Spanish].
20. SABINO M., DE SOUZA A.P. Global Sensitivity of Penman–Monteith Reference Evapotranspiration to Climatic Variables in Mato Grosso, Brazil. Earth. **4**, 714, **2023**.
21. ABDEL F.M.K., ABD E.K.S., ZHANG Z., MERWAD A.R.M.A. Exploring the Applicability of Regression Models and Artificial Neural Networks for Calculating Reference Evapotranspiration in Arid Regions. Sustainability. **15**, 15494, **2023**.
22. ALLEN R.G., PEREIRA L.S., RAES D., SMITH M. Crop Evapotranspiration. Guidelines for Computing Crop Water Requirements. FAO, FAO Irrigation and Drainage. **56**, 300, **1998b**.

23. LIANG Y., FENG D., SUN Z., ZHU Y. Evaluation of Empirical Equations and Machine Learning Models for Daily Reference Evapotranspiration Prediction Using Public Weather Forecasts. Water. **15** (22), 3954, **2023**.
24. OKKAN U., FISTIKOGLU O., ERSOY B.Z., NOORI T.A. Analyzing the uncertainty of potential evapotranspiration models in drought projections derived for a semi-arid watershed. Theoretical and Applied Climatology. **155**, 2329, **2024**.
25. HARGREAVES G.H., SAMANI Z.A. Reference crop evapotranspiration from temperature. Applied Engineering Agriculture. **1** (2), 96, **1985**.
26. TREZZA R. Estimación de la evapotranspiración de referencia a nivel mensual en Venezuela. cuál método utilizar? Bioagro. **20** (2), 89, **2008** [In Spanish].
27. TORO T.A.M., ARTEAGA R.R., VÁZQUEZ P.M.A., IBÁÑEZ C.L.A. Estimation models for the reference evapotranspiration value in the northern Banana zone of Antioquian Uraba (Colombia). Agrociencia. **49**, 821, **2015**.
28. SECRETARÍA DE AGRICULTURA, GANADERÍA, DESARROLLO RURAL, PESCA Y ALIMENTACIÓN (SAGARPA). Agenda Técnica Agrícola de Sinaloa, Segunda Edición; SAGARPA, Mexico City, Mexico, 242 p., **2015** [In Spanish]**.**
29. COMISIÓN NACIONAL DEL AGUA (CONAGUA). Estaciones meteorológicas. https://smn.conagua.gob.mx/es/climatologia/informacion-climatologica/informacion-estadistica-climatologica. **2024** [In Spanish].
30. COMISIÓN NACIONAL DEL AGUA (CONAGUA)– SERVICIO METEOROLÓGICO NACIONAL (SMN). Estaciones meteorológicas (Estación Acaponeta). https://smn.conagua.gob.mx/tools/GUI/sivea_v3/sivea.php. **2024** [In Spanish].
31. OXFORD CAMBRIDGE AND RSA (OCR). Formulae and statistical tables (ST1), 8 p., **2022**.
32. GALINDO R.J.G., ALEGRÍA H. Toxic effects of exposure to pesticides in farm workers in Navolato, Sinaloa (Mexico). Revista Internacional de Contaminación Ambiental. **34** (3), 505, **2018**.
33. SECRETARÍA DE AGRICULTURA, GANADERÍA, DESARROLLO RURAL, PESCA Y ALIMENTACIÓN (SAGARPA). Estimación de las exportaciones agroalimentarias a nivel de entidad federativa. Secretaría de Agricultura, Ganadería, Pesca y Acuacultura. **2011** [In Spanish].
34. LLANES C.O. Predictive association between meteorological drought and climate indices in the state of Sinaloa, northwestern Mexico. Arabian Journal of Geoscience, **16**, 79, **2023**.
35. GUIJARRO J.A. Homogenization of climatic series with Climatol. **2018**.
36. ALEXANDERSSON H. A homogeneity test applied to precipitation data. Journal of Climatology. **6**, 661, **1986**.
37. NATIONAL OCEANIC AND ATMOSPHERIC ADMINISTRATION (NOAA). https://downloads.psl.noaa.gov/Datasets/ncep.reanalysis2/Monthlies/gaussian_grid/. **2024**.
38. VARGA H.Z., SZALKA É., SZAKÁL T. Determination of Reference Evapotranspiration Using Penman-Monteith Method in Case of Missing Wind Speed Data under Subhumid Climatic Condition in Hungary. Atmospheric and Climate Science. **12**, 235, **2022**.
39. LEAL L.H.D.C., ROCHA W.F.D.C. Model adequacy checking in homogeneity and stability studies. Journal of Metrology Society of India (MAPAN). **39**, 445, **2023**.
40. ZAR J.H. Biostatistical analysis. Pearson Prentice Hall, Pearson Education. Inc. Upper Saddle River. New Jersey. **2010**.
41. LÓPEZ A.J.E., DÍAZ V.T., WATTS T.T., RODRÍGUEZ J.C., CASTELLANOS V.A.E., PARTIDA R.L., VELÁZQUEZ A.T.J. Evapotranspiración y coeficientes de cultivo de chile Bell en el Valle de Culiacán, México. Terra Latinoamericana. **33**, 209, **2015** [In Spanish].
42. PUGH S., FOSDICK B.K, NEHRING M., GALLICHOTTE E.N., VANDEWOUDE S., WILSON A. Estimating cutoff values for diagnostic tests to achieve target specificity using extreme value theory. BMC Medical Research Methodology. **24**, 30, **2024**.
43. BRESSANE A., SIMINSKI A., GURJON G.I., PERES M.C., SCOFANO G.C., DOS SANTOS G.A.L., SILVA M.B, DE CASTRO L.C., GALANTE N.G. Prioritization of key indicators for the classification of successional stages in regenerating subtropical Atlantic Forest, Southern Brazil: a proposal based on multivariate order statistics. Environment Systems and Decisions. **43**, 232, **2023**.
44. LLANES C.O., ESTRELLA G.R.D., PARRA G.R.E., GUTIÉRREZ R.O.G., ÁVILA D.J.A., TROYO D.E. Modeling yield of irrigated and rainfed bean in central and southern Sinaloa state, Mexico, based on essential climate variables. Atmosphere. **15** (5), 573, **2024**.
45. FENG Y., JIA Y., CUI N., ZHAO L., LI C., GONG D. Calibration of Hargreaves model for reference evapotranspiration estimation in Sichuan basin of southwest China. Agricultural Water Management. **181** (2), 1, **2017**.
46. GU X., LONG A., HE X., WANG H., LAI X., PANG N., LIU H., YU H. Response of runoff to climate change in the Manas River Basin flow-producing area, Northwest China. Applied Water Science. **14**, 43, **2024**.
47. KUMAR S., SHARDA R., GOYAL P., SIAG M., KAUR P. Reference Evapotranspiration Modelling Using Artificial Neural Networks Under Scenarios of Limited Weather Data: A Case Study in the Malwa Region of Punjab. Environment Modeling & Assessment. **29**, 589, **2023**.
48. CÓRDOVA M., CARRILLO R.G., CRESPO P., WILCOX B., CÉLLERI R. Evaluation of the Penman–Monteith (FAO 56 PM) Method for Calculating Reference Evapotranspiration Using Limited Data. Mountain Research and Development. **35** (3), 230, **2015**.
49. VALLE J.G.L.C., VOURLITIS G.L., AMORIM C.L.F., DA SILVA P.R., NOGUEIRA J.S., LOBO F.A., ABU R.MD.T.I., RANGEL R.T. Evaluation of FAO-56 Procedures for Estimating Reference Evapotranspiration Using Missing Climatic Data for a Brazilian Tropical Savanna. Water. **13** (3), 1763, **2021**.